Fullerenes

DOI: 10.1002/anie.200802009

Carbon Pyramidalization in Fullerene Cages Induced by the Endohedral Cluster: Non-Scandium Mixed Metal Nitride Clusterfullerenes**

Shangfeng Yang, Alexey A. Popov, and Lothar Dunsch**

Metal nitride clusterfullerenes (NCFs) represent a special class of endohedral fullerenes with an encaged trimetallic nitride cluster.[1] One of the characteristic features of the NCFs with homogeneous M_3N clusters is that the structure of the cluster is determined by its size which varies with the radius of the involved metal.[2,3] The mixed metal nitride clusterfullerenes (MMNCFs), that is, the nitride clusterfullerenes with different metals mixed in the encaged nitride, are recognized as a small group within the NCF family.[1,4–15] A noteworthy feature of MMNCFs is that their yields can be higher than those of homogeneous NCFs.[1,4–7,12,13] Such an advantage makes MMNCFs a promising route to boosting the yield of clusterfullerenes, which is often low for homogeneous NCFs incorporating large metal ions. So far a number of MMNCFs have been isolated, including $MSc_2N@C_{80}$ (I_h) (M = Y, Ce, Gd, Tb, Er),[4,8,10–12,15] $M_2ScN@C_{80}$ (I_h) (M = Y, Gd, Er),[4,10–12] $Gd_xSc_{3-x}N@C_{80}$ (D_{5h}) ($x = 1, 2$),[4] $ScYErN@C_{80}$ (I_h),[9] $DySc_2N@C_{76}$,[13] $MSc_2N@C_{68}$(M=Dy, Lu), $Lu_2ScN@C_{68}$.[14] Note that, in all cases, the involvement of Sc was essential to direct the formation of these MMNCFs, because Sc-based NCFs are known to have higher yields, compared to homogeneous NCFs with other metals.[4–16]

An interesting finding revealed in the studies of Sc-based MMNCFs ($M_xSc_{3-x}N@C_{2n}$) is that the yield of the homogeneous Sc-NCFs dominates that of the M-based homogeneous NCFs, for which formation is dramatically suppressed.[4,12] Therefore, an open question to be addressed is the formation of MMNCFs based on two non-Sc metals. In particular, if two metals for which the yield of the homogeneous NCFs is comparable are mixed within one nitride cluster, how would they compete during the formation of MMNCFs and how does the structure of MMNCFs in terms of both the nitride cluster and the carbon cage depend on the composition of the mixed nitride cluster? Herein we report on the synthesis and isolation of $Lu_xY_{3-x}N@C_{80}$ (isomeric structure I, $x = 1, 2$)—the first MMNCFs without the involvement of Sc, with the synthesis of $Lu_xSc_{3-x}N@C_{80}$ (I, $x = 1, 2$) also studied for comparison. The isolated MMNCFs are characterized by UV/Vis-NIR, FTIR, and ^{13}C NMR spectroscopies and the dependence of their spectroscopic properties on the encaged cluster is studied. DFT calculations are also performed to address the effect of the size of the encaged cluster on the structure of the MMNCFs especially with respect to the carbon cage.

In this work, lutetium and yttrium are chosen because the radii of their trivalent ions are similar (0.85 and 0.90 Å,[2,17] respectively) and the yield of the homogeneous $Lu_3N@C_{80}$ is only approximately 1.9 times higher than that of $Y_3N@C_{80}$ (see Supporting Information S1). As neither have partially filled f-shell electrons, their ^{13}C NMR spectroscopic characterization is facilitated. The synthesis of $Lu_xY_{3-x}N@C_{80}$ ($x = 1$, 2) by the "reactive gas atmosphere"[18] method is similar to that of the previously reported $Gd_xSc_{3-x}N@C_{80}$.[4,12] Figure 1 shows a typical chromatogram of a $Lu_xY_{3-x}N@C_{2n}$ fullerene extract mixture obtained under the optimized condition (molar ratio of Lu:Y:C = 1:1:15). The dominant fraction A (t_{ret} = 30.7–33.1 min) is correlated to $Lu_xY_{3-x}N@C_{80}$ (I, $x = 0$–3, hereafter the label "I" for the isomeric structure is omitted for clarity unless specified) according to the mass spectrometric (MS) analysis, with the abundance up to 95% of all the fullerene products. For comparison, the total yield of $Lu_xY_{3-x}N@C_{80}$ ($x = 1, 2$) is approximately 5.4 times lower than that of $Lu_xSc_{3-x}N@C_{80}$ ($x = 1, 2$) which we isolated more recently (the results will be reported elsewhere; see Supporting Information S1), highlighting the role of Sc in promoting the formation of $Lu_xSc_{3-x}N@C_{80}$. Furthermore, because the retention times of $Lu_3N@C_{80}$ and $Y_3N@C_{80}$ are very close, these two products as well as $Lu_xY_{3-x}N@C_{80}$ ($x = 1, 2$) overlap in fraction A. As a result the four possible structures of $Lu_xY_{3-x}N@C_{80}$ ($x = 0$–3) co-elute in one fraction, which is narrower than that of $Lu_xSc_{3-x}N@C_{80}$ ($x = 0$–3) (see Supporting Information S1). As a result, the isolation of

[*] Prof. Dr. S. Yang, Dr. A. A. Popov, Prof. Dr. L. Dunsch
Group of Electrochemistry and Conducting Polymers
Leibniz-Institute for Solid State and Materials Research (IFW) Dresden
01171 Dresden (Germany)
Fax: (+49) 351-4659-811
E-mail: sfyang@ustc.edu.cn
l.dunsch@ifw-dresden.de
Prof. Dr. S. Yang
Hefei National Laboratory for Physical Sciences at Microscale &
Department of Materials Science and Engineering
University of Science and Technology of China
Hefei 230026 (China)
Fax: (+86) 551-3601-750
Dr. A. A. Popov
Department of Chemistry
Moscow State University
Leninskiye Gory, 119992 Moscow (Russia)

[**] We cordially thank K. Leger, S. Schiemenz, and F. Ziegs for their technical assistance. S.Y. thanks the University of Science and Technology of China (USTC) for Startup funding (No.: ZC9850290028). Financial support for A.P. from DAAD and AvH is gratefully acknowledged.

Supporting information for this article is available on the WWW under http://dx.doi.org/10.1002/anie.200802009.

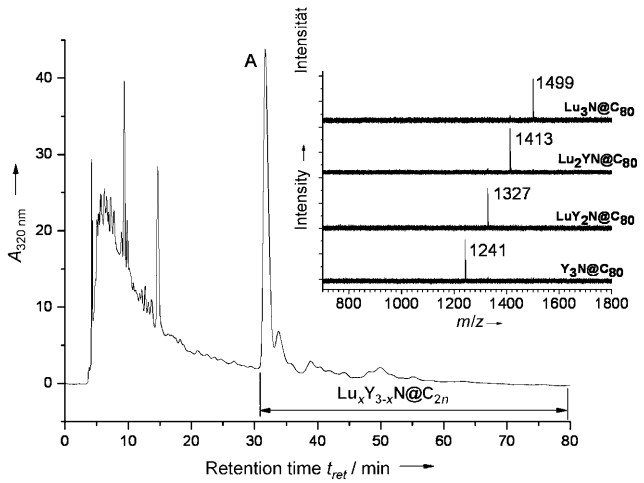

Figure 1. Chromatogram of the $Lu_xY_{3-x}N@C_{2n}$ fullerene extract mixture, synthesized by the "reactive gas atmosphere" method (combination of two 4.6×250 mm Buckyprep columns; flow rate 1.6 mL min^{-1}; injection volume 100 μL; toluene as eluent (mobile phase); 40 °C). Fraction A consists of $Lu_xY_{3-x}N@C_{2n}$ (I; $x=0$–3). Inset: Positive ion laser desorption time-of-flight (LD-TOF) mass spectrum of $Lu_xY_{3-x}N@C_{2n}$ ($x=0$–3) isolated from fraction A.

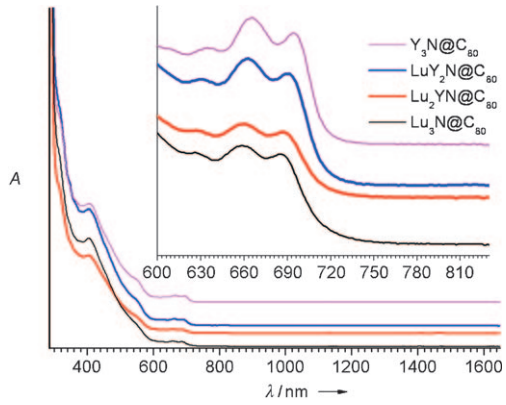

Figure 2. UV/Vis-NIR spectra of $Lu_xY_{3-x}N@C_{2n}$ (I; $x=0$–3) dissolved in toluene. The inset shows the enlarged spectral range (600–830 nm).

Table 1: Electronic absorption data of $Lu_xY_{3-x}N@C_{80}$ ($x=0$–3) MMNCFs.

x	Product	Mass number (m/z)	UV/Vis-NIR absorption peaks (nm)	Onset [nm]	Band gap[a] [eV]
0	$Y_3N@C_{80}$	1241	407, 549, 633, 665, 694	786	1.58
1	$LuY_2N@C_{80}$	1317	403, 549, 630, 662, 690	793	1.56
2	$Lu_2YN@C_{80}$	1413	403, 548, 627, 659, 687	797	1.56
3	$Lu_3N@C_{80}$	1499	403, 548, 626, 658, 685	807	1.54

[a] band-gap (eV) ≈ 1240/onset (nm).

$Lu_xY_{3-x}N@C_{80}$ ($x=1$, 2) is even more laborious than for any Sc-based MMNCFs($M_xSc_{3-x}N@C_{80}$, $x=1$, 2).[4,12] The successful isolation of $Lu_xY_{3-x}N@C_{80}$ ($x=1$, 2) has been accomplished by three-step HPLC, including recycling HPLC in the last two steps of the isolation (see Supporting Information S2 for the detailed isolation procedure). The high purity (≥ 99 %) of the MMNCFs was confirmed by laser-desorption time-of-flight (LD-TOF) MS analysis (inset of Figure 1).

With the successful isolation of $Lu_xY_{3-x}N@C_{80}$ ($x=1$, 2), the relative yield of $Lu_xY_{3-x}N@C_{80}$ ($x=0$–3) has been estimated, according to the integrated area of the corresponding peak in HPLC. Under the optimized synthesis condition (a molar ratio of Lu/Y/C = 1:1:15), the ratio of the yield of $Y_3N@C_{80}/LuY_2N@C_{80}/Lu_2YN@C_{80}/Lu_3N@C_{80}$ is 2.3:4.6:3.6:1 (see Supporting Information S3), as opposed to the 1:3:3:1 ratio that would be expected for an unbiased statistical distribution. In particular, the yield of $LuY_2N@C_{80}$ is ca. 1.3 times that of $Lu_2YN@C_{80}$, and the yield of $Y_3N@C_{80}$ is ca. 2.3 times that of $Lu_3N@C_{80}$. This is especially remarkable as it is the reverse of the relative yields for the synthesis of homogeneous NCFs using pure Lu_2O_3 or Y_2O_3 (see Supporting Information S1). Moreover, according to the integrated area of the corresponding peak in HPLC chromatograms, the yield of the $Lu_xY_{3-x}N@C_{80}$ (I) mixture is ca 1.5 and 2.8 times higher than that of the homogeneous $Lu_3N@C_{80}$ (I) and $Y_3N@C_{80}$ (I), respectively. These results indicate the enhancement of the yield upon the formation of MMNCFs and show that a complicated competition effect takes place when two metals with comparable ionic radii are mixed to form the MMNCFs.

The UV/Vis-NIR spectra of the isolated $Lu_xY_{3-x}N@C_{80}$ ($x=0$–3) dissolved in toluene are shown in Figure 2, and their characteristic absorption data are summarized in Table 1. The overall absorption features of $Lu_xY_{3-x}N@C_{80}$ ($x=0$–3) are almost identical, with subtle shifts of the the bands. Their absorption onsets are also quite close, indicating comparable optical band-gaps (1.58–1.54 eV, see Table 1). All these results point to the close resemblance of their electronic properties, which can be understood by the similarity of Lu^{3+} and Y^{3+} in terms of their ionic radii and the HPLC retention behaviour discussed above.[2] This is, however, not the case for $Lu_xSc_{3-x}N@C_{80}$ (I) as well as for other $M_xSc_{3-x}N@C_{80}$ (I; M = Y, Gd, Er) MMNCFs,[4,10,12] which exhibit considerable variations in their absorption spectra with the change of the encaged cluster, including an increase in the bandgap and an increase in the resolution of the absorption pattern with a higher number of lanthanide atoms in the cluster.[4,10,12]

The FTIR spectra of $Lu_xY_{3-x}N@C_{80}$ ($x=0$–3) in comparison to those of $Lu_xSc_{3-x}N@C_{80}$ ($x=0$–3) shown in Figure 3 clearly indicate the identity of their tangential and radial cage vibrational modes, which are virtually identical to those of other $M_3N@C_{80}$ (I) (M = Sc, Y, Gd, Tb, Dy, Ho, Er, Tm).[1–4,12] This result enables us to assign the same cage isomer, that is, C_{80}:7 with I_h symmetry,[1,2] to all $Lu_xY_{3-x}N@C_{80}$ ($x=0$–3) MMNCFs studied in this work, as well as to $Lu_xSc_{3-x}N@C_{80}$ ($x=1$–2). The anti-symmetric M–N stretching vibrational modes (ν_{M-N}), which appear as the most intense low-energy IR lines in the region of 600–800 cm^{-1},[1–4,12,19a] are more characteristic for a given NCF. Unlike the homogeneous NCFs, in which the anti-symmetric M–N stretching mode is two-fold degenerate, the lower molecular symmetry in MMNCFs results in the splitting of this mode.[4,12] However, the magnitude of splitting is quite different for $Lu_xY_{3-x}N@C_{80}$ and $Lu_xSc_{3-x}N@C_{80}$ ($x=0$–3). The ν_{M-N} frequencies in $Lu_3N@C_{80}$ and $Y_3N@C_{80}$ are quite close, and similar spectral

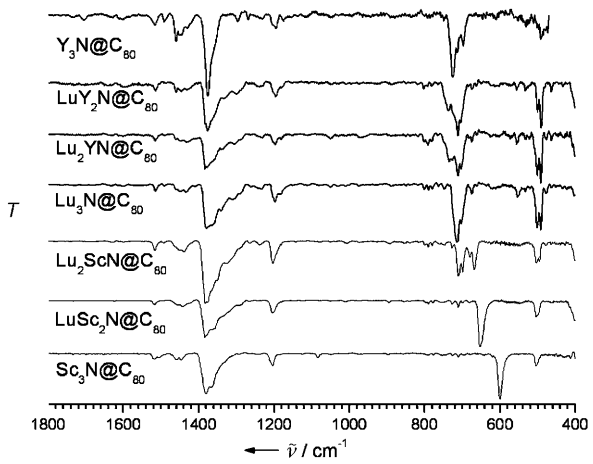

Figure 3. FTIR spectra of $Lu_xY_{3-x}N@C_{2n}$ and $Lu_xSc_{3-x}N@C_{80}$ ($x=0$–3).

patterns are also observed for the corresponding MMNCFs (Figure 3, Table 2), with the only indication of the splitting being the somewhat broader bands in $Lu_xY_{3-x}N@C_{80}$ ($x=1, 2$). A more complex behaviour of the ν_{M-N} mode is observed for $Lu_xSc_{3-x}N@C_{80}$ ($x=0$–3). $Lu_2ScN@C_{80}$ exhibits significant splitting (main components are observed at 668 and 710 cm^{-1}), while only one band (at 652 cm^{-1}) is found in $LuSc_2N@C_{80}$. The latter frequency is different from both $Sc_3N@C_{80}$ (599 cm^{-1}) and $Lu_3N@C_{80}$ (714 cm^{-1}). Interpretation of these data is straightforward if M–N bondlengths in DFT-optimized clusterfullerenes are analyzed (Table 2). As the ionic radii of Lu^{3+} and Y^{3+} are close, they have similar M–N bondlengths (however, Y is still somewhat larger, and the cluster in $Y_3N@C_{80}$ is predicted to be slightly pyramidal, the N being 0.083 Å displaced out of Y_3 plane). As a result, there are marginal variations in Lu–N and Y–N bond lengths in $Lu_xY_{3-x}N@C_{80}$ as compared to homogeneous NCFs, and the splitting of ν_{M-N} is small. The difference of ionic radii of Sc^{3+} and Lu^{3+} is rather large, and Lu–N bonds in $Lu_xSc_{3-x}N@C_{80}$ ($x=1,2$) are elongated at the expense of considerable shortening of Sc–N bonds. As a result, ν_{Sc-N} increases from 599 cm^{-1} in $Sc_3N@C_{80}$ to 652 cm^{-1} in $LuSc_2N@C_{80}$ to 710 cm^{-1} in $Lu_2ScN@C_{80}$, while ν_{Lu-N} decreases from 714 cm^{-1} in $Lu_3N@C_{80}$ to 668 cm^{-1} in $Lu_2ScN@C_{80}$ to 652 cm^{-1} in $LuSc_2N@C_{80}$.[19b] Similar changes in ν_{Sc-N} and ν_{M-N} were observed for other $M_xSc_{3-x}N@C_{80}$ (M = Gd, Y, Er) and in $Lu_xSc_{3-x}N@C_{68}$.[4,12,14]

Table 2: Characteristic structural and spectroscopic data of $Lu_xY_{3-x}N@C_{80}$ MMNCFs ($Lu_xSc_{3-x}N@C_{80}$ MMNCFs are also given for comparison).

Product	ν_{M-N}[a] [cm^{-1}]	d_{Lu-N} [Å][b]	d_{M-N} [Å][c]	^{13}C NMR shift [ppm]
$Y_3N@C_{80}$	698, 714, 725	–	2.060	138.04, 144.44
$LuY_2N@C_{80}$	705, 713, 717, 723, 736	2.054	2.064, 2.065	137.95, 144.41
$Lu_2YN@C_{80}$	703, 712, 726, 735	2.058, 2.059	2.069	137.66, 144.22
$Lu_3N@C_{80}$	703, 714	2.062	–	137.39, 144.02
$Lu_2ScN@C_{80}$	668, 680, 699, 710	2.104, 2.107	1.945	137.12, 143.99
$LuSc_2N@C_{80}$	652	2.147	1.988, 1.993	136.90, 143.99
$Sc_3N@C_{80}$	599	–	2.034	136.87, 144.18

[a] ν_{M-N} represents the anti-symmetric stretching vibrational frequency of M–N; [b] d_{Lu-N} represents the DFT-predicted bond length of Lu–N; [c] d_{M-N} represents the DFT-predicted bond length of M–N (Y–N or Sc–N).

The 125 MHz ^{13}C NMR spectra of $Lu_xY_{3-x}N@C_{80}$ and $Lu_xSc_{3-x}N@C_{80}$ ($x=0$–3) obtained at room temperature exhibit two narrow lines with chemical shifts of 137–138 and 144–145 ppm, respectively (see Figure 4 and Table 2). The intensity ratio of these two lines is 1: 3, which is characteristic for NCFs with the C_{80} (I_h) cage isomer.[4,6,7] Significantly, the ^{13}C NMR lines show appreciable downshifts with the shrinking of the encaged nitride cluster, that is, in the order of $Y_3N@C_{80}\rightarrow LuY_2N@C_{80}\rightarrow Lu_2YN@C_{80}\rightarrow Lu_3N@C_{80}\rightarrow Lu_2ScN@C_{80}\rightarrow LuSc_2N@C_{80}$ (however, $Sc_3N@C_{80}$ exhibits some deviation). Such a systematic shift of the ^{13}C NMR lines with the change of the composition of the encaged cluster has not previously been reported for NCFs. A further analysis on the ^{13}C NMR spectra is presented below.

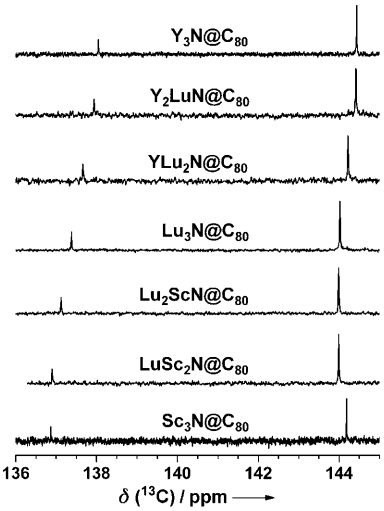

Figure 4. The 125 MHz ^{13}C NMR spectra of $Lu_xY_{3-x}N@C_{80}$ and $Lu_xSc_{3-x}N@C_{80}$ ($x=0$–3) in CS_2/d_6-Acetone at room temperature.

In the analysis of the ^{13}C NMR spectra of the empty fullerenes it was established that ^{13}C shifts correlate with the pyramidalization of the carbon atoms as quantified in terms of the π-orbital axis vector (POAV) analysis.[20,21] To understand the observed shift of the ^{13}C NMR lines of $M_3N@C_{80}$, we performed DFT calculations of the molecular structures of all NCFs studied in this work focusing on the curvature of the carbon cage induced by the cluster (see Supporting information S4).[22] There are two different types of carbon atoms within the C_{80}:I_h cage—the pyrene-type carbon atoms (triple-hexagon junctions, THJs, which correlate to the NMR line at a lower shift of 137–138 ppm) and the corannulene-type carbon atoms (pentagon/hexagon/hexagon junctions (PHHJs) which correlate to the NMR line at a higher shift,

around 144 ppm).[1,5,7a] It is known from experimental data, as well as from the calculations reported herein, that coordination to the endohedral metal increases pyramidalization of the carbon atoms.[7b] With respect to this, it should be pointed out that THJs are originally more planar, and hence their pyramidalization appears to be less energetically favored than that of PHHJs. One consequence of this point is the avoidance of additional THJs in the chemical derivatization of higher fullerenes.[23]

Figure 5a–c illustrates the enlarged view of the metal-coordinated hexagon within DFT-predicted C_3 isomers of $M_3N@C_{80}$ (M = Sc, Lu, Y).[24] In $Sc_3N@C_{80}$ the Sc atom is significantly displaced from the center of the hexagon, being

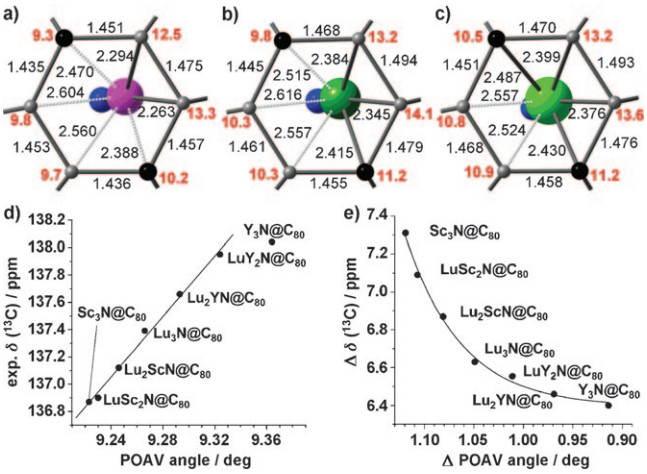

Figure 5. Enlarged view of the metal-coordinated hexagon in the C_3 isomers of (a) $Sc_3N@C_{80}$, (b) $Lu_3N@C_{80}$, and (c) $Y_3N@C_{80}$ with DFT-optimized interatomic distances [Å, in black] and POAV angles [°, in red]. The THJs are highlighted as black spheres. (d) Correlation between the experimental ^{13}C chemical shifts of THJs of $Lu_xY_{3-x}N@C_{80}$ and $Lu_xSc_{3-x}N@C_{80}$ ($x = 0$–3) and the averaged POAV angles of carbon atoms on THJs. (e) Correlation of Δ(^{13}C chemical shift) and Δ(POAV angle) of $Lu_xY_{3-x}N@C_{80}$ and $Lu_xSc_{3-x}N@C_{80}$ (x = 0–3).

coordinated to the pentagon/hexagon edge, whereas, with the increase in cluster size to Lu_3N and further to Y_3N, the metal is shifted in the cage towards the center of the hexagon.[25] Thus, the Sc atoms in $Sc_3N@C_{80}$ are presumably coordinated to the PHHJs, as could be anticipated based on energetic considerations. However, the larger sizes of the Lu_3N and Y_3N clusters preclude the same type of coordination as for Sc_3N, forcing Lu and Y metals to be coordinated to the THJs as well. Therefore, the average POAV angle of THJs in $M_3N@C_{80}$ increases with increasing cluster size. This trend is evident as the perfect correlation of the POAV angle of THJs to their ^{13}C chemical shifts (as can be seen in Figure 5d). As the total curvature of the cage should be preserved, the average POAV angle of PHHJs decreases to compensate for the increased POAV angle of THJs. However, the magnitude of the changes of POAV(PHHJ) is smaller in view of the three-to-one ratio of PHHJs to THJs. This behavior also correlates with the smaller magnitude of changes to the ^{13}C chemical shift of PHHJs (ca 0.5 ppm), compared to that for THJs (ca 1.5 ppm). Finally, although the POAV(PHHJ) shows a weaker correlation with ^{13}C shifts (see Supporting information S5), Δ(POAV) exhibits a good correlation with Δ(^{13}C shift) (Figure 5e). This result is a consequence of the pyramidalization of the carbon atoms being dependent on the encaged mixed metal nitride cluster. With the enlargement of the cluster size from Sc_3N via Lu_3N to Y_3N, the larger metal atoms (Lu and Y) "move" closer to the center of the hexagon and hence lead to the increase in local curvature, as the coordination of the metal is distributed more evenly over the cage atoms, resulting in the increase of the pyramidalization of pyrene-type carbon atoms (that is, the increase of the average POAV angle of THJs).

In summary, we have successfully synthesized and isolated the first MMNCFs without the involvement of Sc—$LuY_2N@C_{80}$ and $Lu_2YN@C_{80}$. The UV/Vis-NIR spectroscopic study reveals a similarity in electronic properties to their respective analogous homogeneous NCFs ($Y_3N@C_{80}$ and $Lu_3N@C_{80}$) in terms of the HOMO–LUMO absorption bands and optical band-gap. The vibrational structures of $LuY_2N@C_{80}$ and $Lu_2YN@C_{80}$ are found to resemble those of $Lu_3N@C_{80}$ and $Y_3N@C_{80}$ in terms of the frequencies of ν_{M-N} and cage vibrational modes as indicated by FTIR spectroscopic characterization. The ^{13}C NMR spectroscopic study of $LuY_2N@C_{80}$ and $Lu_2YN@C_{80}$ indicates two sharp lines. A systematic comparison of the ^{13}C NMR chemical shifts of $Lu_xY_{3-x}N@C_{80}$ ($x = 0$–3) with those of $Lu_xSc_{3-x}N@C_{80}$ ($x = 0$–3) indicates that the two NMR signals undergo appreciable downshifts with shrinking cluster size, while the gap between the two signals decreases. This result is interpreted by the correlation of the shifts of the ^{13}C NMR lines with the pyramidalization of the carbon atoms as analyzed in detail by DFT calculations. With increasing cluster size, the larger metal atoms move to the center of the hexagons of the carbon cage, and this leads to the increase in pyramidalization of the pyrene-type carbon atoms. As the first report of the change of pyramidalization of the carbon atoms induced by the encaged cluster, this study provides a new insight to the carbon cage structure of endohedral fullerenes.

Experimental Section

General procedures for the synthesis of $Lu_xY_{3-x}N@C_{80}$ ($x = 1, 2$) are similar to those used for synthesizing $Gd_xSc_{3-x}N@C_{80}$ (I; $x = 1, 2$) reported elsewhere.[4,12,18] A mixture of Lu_2O_3 and Y_2O_3 and graphite powder with an optimized molar ratio of Lu:Y:C = 1:1:15 was subjected to DC-arc discharging by a modified Krätschmer-Huffman DC-arc discharging method with the addition of NH_3 (20 mbar). Clusterfullerene separation was performed by a three-step HPLC as described in detail in Supporting Information S2. The purity of the isolated product was further checked by LD-TOF MS analysis running in both positive and negative ion modes (Biflex III, Bruker, Germany). Sample preparation and experimental details for UV/Vis-NIR and FTIR spectroscopic measurements were described previously.[4,12–14] The ^{13}C NMR spectroscopic study was performed at 125 MHz in a multiprobe head PH 1152Z on an Avance 500 spectrometer (Bruker) at room temperature in carbon disulfide

solution with [D_6]acetone as a lock. DFT calculations were described previously.[4,12–14]

Received: April 29, 2008
Published online: September 24, 2008

Keywords: cluster compounds · fullerenes · nitrides · NMR · vibrational spectroscopy

[1] For recent reviews, see a) L. Dunsch, S. Yang, *Small* **2007**, *3*, 1298 – 1320; b) L. Dunsch, S. Yang, *Phys. Chem. Chem. Phys.* **2007**, *9*, 3067 – 3081.
[2] S. F. Yang, S. Troyanov, A. Popov, M. Krause, L. Dunsch, *J. Am. Chem. Soc.* **2006**, *128*, 16733 – 16739.
[3] A. Popov, L. Dunsch, *J. Am. Chem. Soc.* **2007**, *129*, 11835 – 11849.
[4] S. F. Yang, A. Popov, M. Kalbac, L. Dunsch, *Chem. Eur. J.* **2008**, *14*, 2084 – 2092.
[5] S. Stevenson, P. W. Fowler, T. Heine, J. C. Duchamp, G. Rice, T. Glass, K. Harich, E. Hajdu, R. Bible, H. C. Dorn, *Nature* **2000**, *408*, 427 – 428.
[6] a) M. M. Olmstead, A. de Bettencourt-Dias, J. C. Duchamp, S. Stevenson, H. C. Dorn, A. L. Balch, *J. Am. Chem. Soc.* **2000**, *122*, 12220 – 12226; b) R. M. Macfarlane, D. S. Bethune, S. Stevenson, H. C. Dorn, *Chem. Phys. Lett.* **2001**, *343*, 229 – 234; c) I. N. Ioffe, A. S. Ievlev, O. V. Boltalina, L. N. Sidorov, H. C. Dorn, S. Stevenson, G. Rice, *Int. J. Mass Spectrom.* **2002**, *213*, 183 – 189.
[7] a) E. B. Iezzi, J. C. Duchamp, K. R. Fletcher, T. E. Glass, H. C. Dorn, *Nano Lett.* **2002**, *2*, 1187 – 1190; b) S. Stevenson, H. M. Lee, M. M. Olmstead, C. Kozikowski, P. Stevenson, A. L. Balch, *Chem. Eur. J.* **2002**, *8*, 4528 – 4535.
[8] X. L. Wang, T. M. Zuo, M. M. Olmstead, J. C. Duchamp, T. E. Glass, F. Cromer, A. L. Balch, H. C. Dorn, *J. Am. Chem. Soc.* **2006**, *128*, 8884 – 8889.
[9] N. Chen, E. Y. Zhang, C. R. Wang, *J. Phys. Chem. B* **2006**, *110*, 13322 – 13325.
[10] N. Chen, L. Z. Fan, K. Tan, Y.Q Wu, C. Y. Shu, X. Lu, C. R. Wang, *J. Phys. Chem. C* **2007**, *111*, 11823 – 11828.
[11] N. Chen, E. Zhang, K. Tan, C. R. Wang, X. Lu, *Org. Lett.* **2007**, *9*, 2011 – 2013.
[12] S. F. Yang, M. Kalbac, A. Popov, L. Dunsch, *ChemPhysChem* **2006**, *7*, 1990 – 1995.
[13] S. F. Yang, A. Popov, L. Dunsch, *J. Phys. Chem. B* **2007**, *111*, 13659 – 13663.
[14] S. F. Yang, A. Popov, L. Dunsch, *Chem. Commun.* **2008**, 2885 – 2887.
[15] S. Stevenson, C. J. Chancellor, H. M. Lee, M. M. , A. L. Balch, *Inorg. Chem.* **2008**, *47*, 1420 – 1427.
[16] Note that in Ref. [7a] the formation of $Lu_{3-x}A_xN@C_{80}$ ($x = 0$–2; A = Gd, Ho) was detected by mass spectrometric measurements, but the corresponding MMNCFs have not been isolated.
[17] N. N. Greenwood, A. Earnshaw, *Chemistry of the Elements*, Pergamon, Oxford, **1984**.
[18] L. Dunsch, M. Krause. J. Noack, P. Georgi, *J. Phys. Chem. Solids* **2004**, *65*, 309 – 315.
[19] a) For $M_3N@C_{80}$, the large vibrational density of states generally results in the mixing of the anti-symmetric M–N stretching mode of the cluster with the cage modes of the same symmetry. As a result, the M–N vibrational mode within $M_3N@C_{80}$ is generally split between several vibrations in the range of up to 30 cm^{-1} with contributions of 20–40 % for each vibration. Each vibration of $M_3N@C_{80}$ with a higher M–N contribution has a rather higher intensity, and therefore several bands are usually detected in the range of the anti-symmetric M–N stretching mode. This kind of mixing is not caused by specific cluster-cage interactions but results solely from the coincidence of the vibrational frequencies of the cluster and the cage, and hence it may be different for different $M_3N@C_{80}$ (depending on which particular cage modes coincide with the frequency of a given cluster); b) The coincidence of ν_{Lu-N} and ν_{Sc-N} in $LuSc_2N@C_{80}$ is accidental.
[20] T. Heine, M. Buhl, P. W. Fowler, G. Seifert, *Chem. Phys. Lett.* **2000**, *316*, 373 – 380.
[21] G. Y. Sun, M. Kertesz, *J. Phys. Chem. A* **2001**, *105*, 5212 – 5220.
[22] POAV values were calculated for all 80 carbon atoms in each $Lu_xY_{3-x}N@C_{80}$ and $Lu_xSc_{3-x}N@C_{80}$ and were then averaged for THJs (20 atoms) and PHHJs (60 atoms).
[23] N. B. Shustova, I. V. Kuvychko, R. D. Bolskar, K. Seppelt, S. H. Strauss, A. A. Popov, O. V. Boltalina, *J. Am. Chem. Soc.* **2006**, *128*, 15793 – 15798.
[24] Note that there are several conformers for each clusterfullerene with different orientation of the cluster inside. The lowest energy structures have C_3 and C_s symmetries, and the relative stability of the C_3-symmetric structure with respect to C_s configuration increases with increasing cluster size in the order Sc_3N(4.6 kJ mol^{-1})–Lu_3N(5.0 kJ mol^{-1})–Y_3N(8.8 kJ mol^{-1}). Similarly, several structures can be obtained for the mixed clusters by replacing one or two metal atoms in either C_3 or C_s conformers and, likewise, it is found that the lowest energy structures are always based on C_3-derived isomers. With this respect, analysis given in this work is based on C_3-derived structures.
[25] That is, in $Sc_3N@C_{80}$ the Sc atom is coordinated to the pentagon/hexagon edge, while in $Y_3N@C_{80}$ it would be more correct to say that Y is coordinated to the whole hexagon (although it is still somewhat displaced from the center).

